

## **DETECTION OF INCIPIENT STRESS CORROSION CRACKING DAMAGE IN PRIMARY LOOP PIPING USING FIBER OPTIC STRAIN GAGES**

***Benjamin K. Jackson, Ph.D.***

***David Bosko, P.E.***

***Michael T. Cronin, P.E.***

***Jonnathan L.W. Warwick, Ph.D.***

*Intertek AIM*

*601 W. California Ave., Sunnyvale, CA 94086, USA*

***James J. Wall***

*Electric Power Research Institute*

*1300 W. T. Harris Blvd., Charlotte, NC 28221, USA*

### **ABSTRACT**

Current nondestructive examination (NDE) technology detection capabilities limit our ability to detect stress corrosion cracking (SCC) damage until it has progressed significantly. This work describes the continued development of an in-situ monitoring technique to detect and characterize mechanical damage caused by SCC, allowing the detection of the incipient stages of damage to components/piping. The application of this study is to prevent failures in the primary cooling loop piping in nuclear plants. The main benefit to the industry will be improved safety and component lifetime assessment with fewer inspections. The technique utilizes high resolution fiber optic strain gages mounted on the pipe outside diameter (OD). This technique has successfully detected changes in the residual stress profile caused by a crack propagating from the pipe inside diameter (ID). The gages have a resolution of  $< 1 \mu\epsilon$ . It has been shown experimentally for different crack geometries that the gages can readily detect the changes of approximately 10-60  $\mu\epsilon$  caused on the OD of the pipe due to crack initiation on the ID. This paper focuses on the latest in the development of the technology. Details of the previous work in this effort may be found in References 1 through 3. A short summary is provided in this paper. The main recent development was the full scale accelerated SCC cracking in boiling magnesium chloride ( $MgCl_2$ ) experiment. In conjunction with experimentation, both 2D and 3D finite element (FEA) models with thermal and mechanical analyses have been developed to simulate the changes in residual stresses in a welded pipe section as a SCC crack progresses.

### **INTRODUCTION**

#### **Background and Motivation**

One of the biggest challenges for the nuclear power industry is SCC in aging materials as plants continue to run beyond their original design lifetimes. This occurs in structural materials of pressurized water reactors (PWR) and boiling water reactors (BWR) primarily in the sensitized heat affected zones (HAZ) of welds. Current NDE technology is limited in its ability to detect

SCC cracks in their incipient stages. Previous laboratory-based studies undertaken by EPRI suggest that component lifetime in the field is more often governed by the initiation and growth of short SCC than by the growth of long (deep) cracks [4]. SCC is especially dangerous as it can propagate rapidly once initiated with little or no change in external environment. The inspection interval for each individual weld may be as long as 10-15 years of operation. This is likely sufficient time for a through wall crack to form from an initiation point that currently is too small to detect. The purpose of this work has been to develop a real time in-situ technique to allow the earliest possible detection of incipient stage damage to components/piping. This is achieved by monitoring the change in residual stress on the pipe OD as an ID SCC crack initiates, using highly sensitive fiber optic strain gages. The technique has gone through proof of concept [1-3], and this work now presents the results from the most realistic damage simulations (both experimental and modeling based) to date. The main benefit to EPRI members will be improved component lifetime assessment with fewer inspections.

## DISCUSSION

### Overview of Monitoring Technology Development to Date

A more complete description of the various stages and experimental methods may be found in References 2 through 4. Firstly, a proof of concept study was conducted on a flat welded plate. A “crack” front was simulated by electrical discharge machining (EDM) that introduced a linear advancing crack front from the weld root towards the crown. A second experiment set used an EDM electrode to simulate a more realistic semielliptical crack front progressing through a circumferential weld in a pipe section. These experiments both showed that there was a measureable and distinct strain response to crack initiation and propagation, independent of temperature change, on the weld crown side (OD for the pipe) of a crack initiated on the opposite side. In an effort to correlate strain response with crack depth, the initial portion of the data for each semielliptical crack front experiment was taken and normalized to remove the time component. Figure 1 shows the strain response data for the central strain gage for the first 5 mm of cut for each of the normalized data sets.

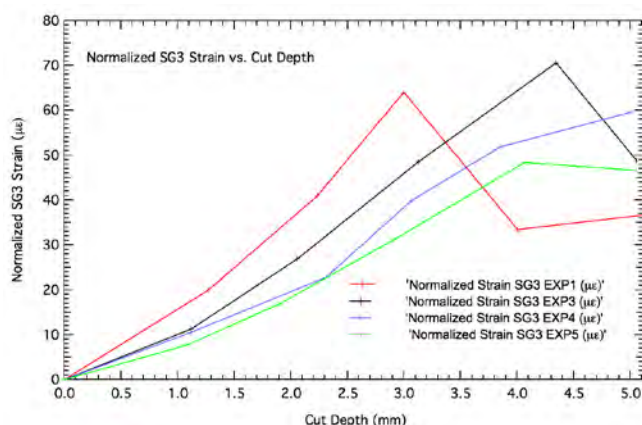


Figure 1: Normalized Strain versus Depth Correlation Elliptical EDM Crack Experiment.

It can be seen that the relationship between cut depth and strain response is approximately linear for the first 3 mm. Experimental limitations prevent constant cut rate beyond this depth. With

further data sets it may be possible to develop a semi-quantitative relationship between crack depth and strain response for a single crack. The presence of multiple, interacting, or branched cracks will likely make this significantly more challenging. The experiments were limited in their ability to accurately simulate an SCC crack, as the cracks produced were not branched, and they did not follow the path of the sensitized region in the HAZ. There were also some equipment limitations that prevented a constant crack growth rate. However, it was considered sufficient to prove the concept that changes in residual stress could be used to monitor for crack initiation.

### Full Scale Boiling $MgCl_2$ Accelerated SCC Experimental Method

This experiment represents the most realistic simulation of SCC cracking to date. The specimen used was, as in the semielliptical EDM experiments, a 12-inch OD 304L pipe section with a 1-inch wall thickness, and a height of 22 inches. There was a single V-groove circumferential weld half way along its length. The experimental method is based on ASTM G36 - 94(2013): “Standard Practice for Evaluating Stress-Corrosion-Cracking Resistance of Metals and Alloys in a Boiling Magnesium Chloride Solution” [5]. This standard uses small test coupons (approximately 0.5-1.0 inch<sup>2</sup>) immersed in boiling  $MgCl_2 \cdot 6H_2O$  in a 1-liter Erlenmeyer flask. The boiling magnesium chloride test is applicable to wrought, cast, and welded stainless steels and related alloys. It is a method for detecting the effects of composition, heat treatment, surface finish, microstructure, and stress on the susceptibility of these materials to chloride stress corrosion cracking [5]. The boiling  $MgCl_2$  solution reacts with the stainless steel to achieve chloride stress corrosion cracking in an accelerated time frame. The experimental method employed here uses a scaled up specimen in the form of the entire pipe section, and an accordingly scaled up volume of corrosive media.

Figure 2 shows a diagram of the experimental set up with an image of the as-built apparatus. Eighteen fiber optic strain gages (SG) and six temperature compensation (TC) gages were evenly spaced around the OD of the pipe spanning the weld.

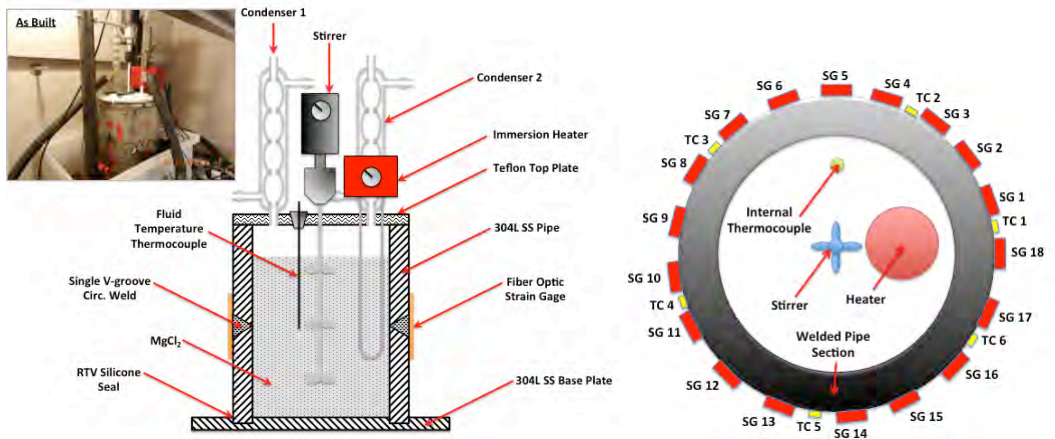


Figure 2: Boiling  $MgCl_2$  SCC Experiment Setup.

An immersion heater with titanium (Ti) coated heating elements is used to initially melt the solid powdered  $MgCl_2 \cdot 6H_2O$  and to maintain it in a boiling molten state. An independent thermocouple is used to monitor the fluid temperature and maintain it at 155°C. The fiber optic strain gages and their associated temperature compensation gages record data at a rate of 10 Hz throughout the

experiment. The external thermocouple records fluid temperature at a rate of 1 Hz. The boiling solution is maintained until through wall cracking is observed or significant cracking is observed in the strain responses. Additional  $\text{MgCl}_2 \cdot 6\text{H}_2\text{O}$  powder is added as necessary to counteract any evaporative fluid losses.

### Full Scale Boiling $\text{MgCl}_2$ Accelerated SCC Results & Discussion

The experiment ran for a total of 12 days before the heater failed, causing the  $\text{MgCl}_2$  solution to solidify. Importantly, the solution in contact with the weld and HAZ area on the ID remained molten throughout the experiment. The apparatus was disassembled and the ID surface of the weld inspected using dye penetrant (DP) to check for indications of cracking around the weld. Figure 3 shows the results of the DP inspection. Indications of cracking were evident in the HAZ regions both above and below the root of the weld pass around almost the entire circumference of the pipe ID.

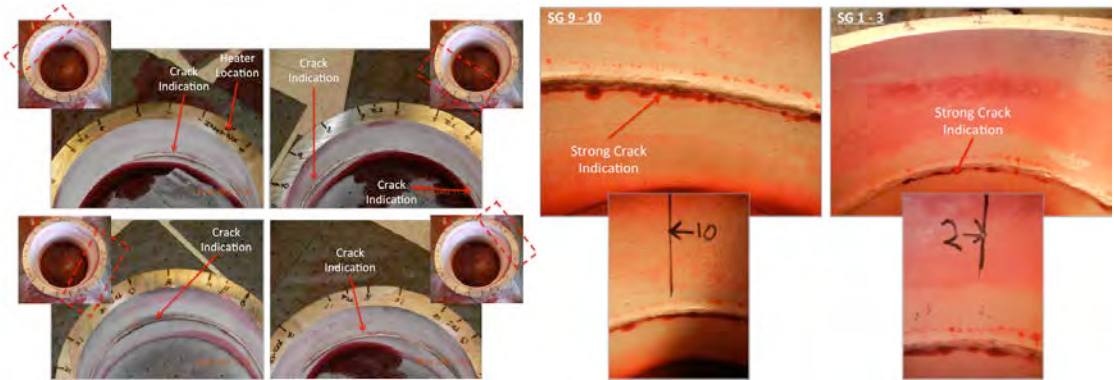


Figure 3: Dye Penetrant Testing Results on Weld ID.

Two regions showing the strongest indications were chosen for detailed metallographic analysis, and the pipe was sectioned to expose the cross section of the welds in these locations. Close-up images of these regions are also shown in Figure 3. The sections were taken underneath SG2 and SG10. SG2 was located close to the heater, and SG10 was approximately opposite SG2, furthest away from the heater. The cross-sections were mounted, ground, polished, and etched (Marbles) according to standard metallographic procedures. Figures 4 and 5 show the as-polished, etched, and a magnified collage of the cracked regions for SG2 and SG10, respectively. It is clear from Figures 4 and 5 that the experiment has successfully generated SCC cracks. Classic branched cracks typical of SCC are clearly visible. In the SG2 region, the cracking extends approximately 50% of the wall. Cracks initiate at the root of the weld in the HAZ, grow along the HAZ, and terminate in the weld metal. This is a typical example of SCC. In this case cracking is both intergranular and transgranular in nature. This result is significant, as it is highly challenging to induce SCC in a large specimen in an accelerated laboratory test.

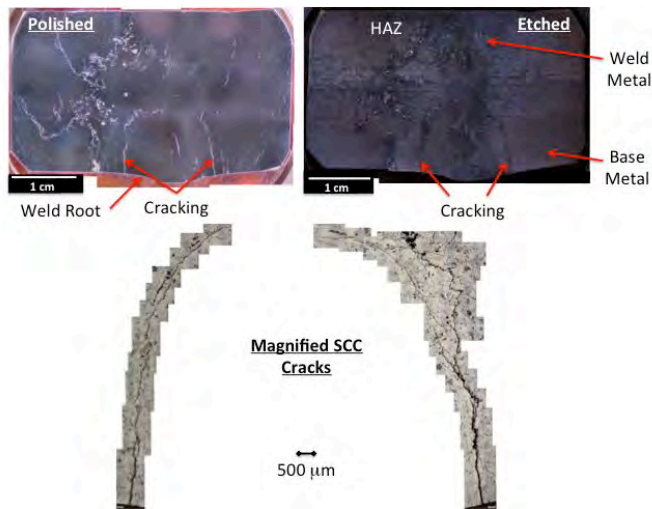


Figure 4: Metallurgical Evaluation of Weld Cross-section at SG2.

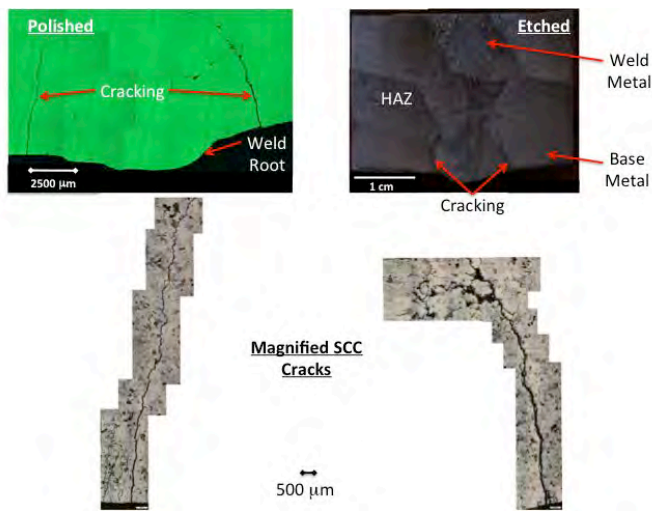


Figure 5: Metallurgical Evaluation of Weld Cross-section at SG10.

The SG and TC data were processed and analyzed upon completion of the experiment. Strain events that were independent of temperature events were identified, and are summarized below:

- Figure 6 shows strain and temperature data for a select time period near the beginning of the run. There is a strain event indicated on all of the SGs simultaneously at time stamp  $105.5 \times 10^3$  s. There are no corresponding temperature responses. This is the first large strain change. The response is characterized by a sharp change in slope for a response of approximate magnitude of approximately  $50 \mu\epsilon$ . This is similar to the EDM experiments. The strain change measured on all gages simultaneously and to similar magnitude. This is the likely initiation point of one or multiple SCCs.



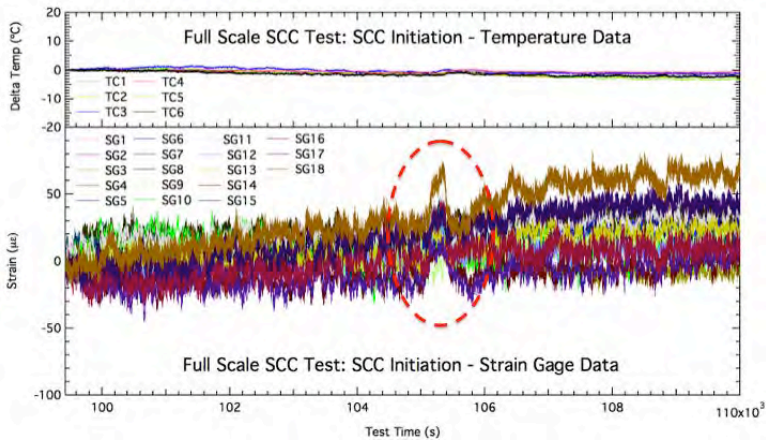


Figure 6: SCC Initiation.

- Figure 7 shows strain and temperature data for a subsequent time period. The plot shows a divergence of SG10 (green) and SG18 (brown) from the baseline strain. This is a more gradual slope change, followed by a steady strain response. SG10 and SG18 are approximately opposite each other around the pipe OD, suggesting that a single cracking event puts one side of the pipe into compression and the other into tension. Given that this is a gradual slope change compared to that observed in Figure 6, this is likely the strain response to steady state crack growth. There are some thermal events also shown on the plot. The drop in temperature likely closed up the SCC crack as indicated by the sharp strain increase in SG10. There is a gradual decrease in temperature throughout the time period, which corresponds to the gradual increase in baseline strain. The data shows interaction of multiple initiating and growing cracks. Unlike the previous EDM tests, it will likely be very challenging to relate strain responses for multiple cracks to location and length. However, sharp changes in slope in the strain response may still be distinguished and flagged as a crack initiation/growth event for further inspection. Multiple other examples of steady state growth were found in the data.

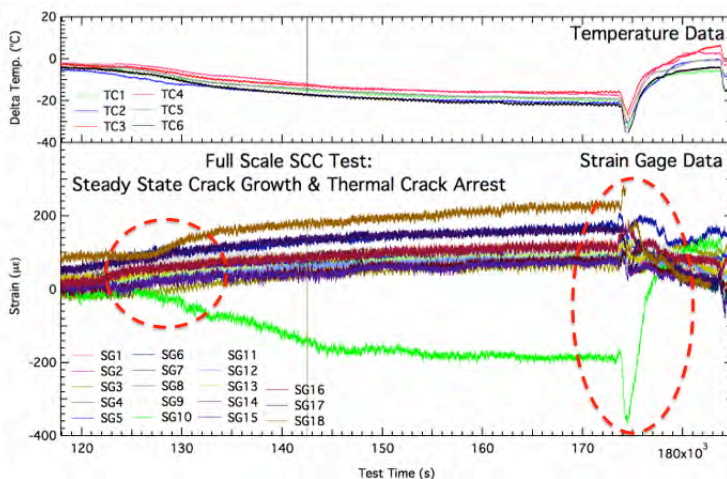


Figure 7: Steady State SCC Growth and Arrest.

- Figure 8 shows strain and temperature data for a subsequent time period. The event at time stamp approximately  $320\text{-}325 \times 10^3$  s shows a sudden strain increase, followed by steady state, then a similar sharp decrease (a “hat shaped” profile). The magnitude was largest at SG10, but was registered on all the other gages. The event could have been a “pop” when the crack progressed through a localized region of lower toughness, and then arrested once it progressed through this region, perhaps passing from HAZ to weld metal or weld bead to weld bead. The hat shaped profile strain event was observed several times after this as the experiment progresses. There is a continued increase in strain over the baseline at SG1 and SG2 as crack progresses. A possible explanation for the resetting of the stress is local deformation at the crack tip.

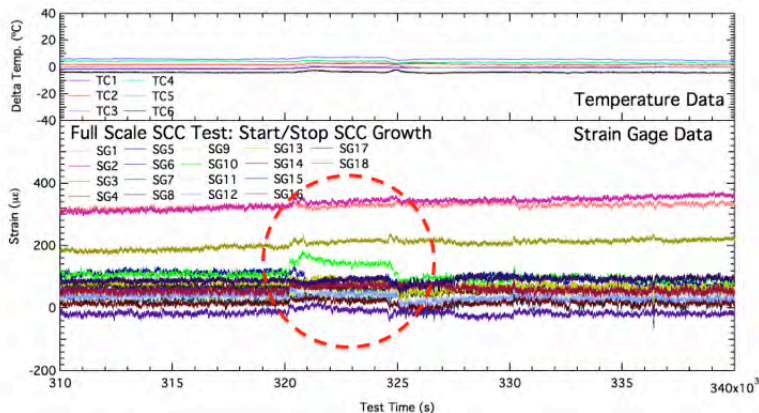


Figure 8: Start/Stop SCC Growth.

## FEA Modeling of Weld Induced Residual Stresses

In order to accurately simulate the real life multi-pass weld process in a full 3D thermo-mechanical model, a 2D thermo-mechanical model was first developed to refine the process of setting up a welding mechanics FEA model. Once the process for analysis was determined and reasonable results were acquired with the 2D analysis, a full 3D model was then created and analyzed. Both models take all non-linearity associated with the welding process into account. These non-linearities include temperature-dependent material properties, moving heat source, material deposition, latent heat, and large deformations.

## Two-Dimensional Thermo Mechanical Analysis

The 2D model was created using 2D axisymmetric elements with a greater mesh density in the area of interest. The initial analysis was set up to include a seven “Lumped Pass” weld model. A lumped pass model is used to reduce computation time. Multiple weld beads are considered as one lumped pass. Heat fluxes for each pass in a layer are added and distributed over the weld elements. A separate heat flux array table was defined for each weld pass. Various thermal analyses were conducted with each time-step result from the thermal analysis used as input conditions for the mechanical analysis. The maximum equivalent stresses were found to be on the order of 45 ksi. This initial 2D analysis helped to define the process of the weld analysis with further refinements to the model to be done using the 3D model and analysis.

### Three-Dimensional Thermo Mechanical Analysis

The 3D analysis includes all the material property data of the 2D study with the added properties of temperature-dependent Poisson's ratio as well as enthalpy. The 3D model was created with thermal brick and pyramid elements. There are a total of 1,216 individual weld volumes. The V-shaped weld groove cross-section is comprised of 32 individual beads. Each of the 32 circumferential weld beads is composed of 38 individual 1-inch nuggets, which, during the analysis, are activated one at a time every 6 seconds to simulate a traveling weld arc. Heat input arrays were created for each of the individual weld nuggets, which are then called on as heat loads as needed. Each array can be customized for a particular ramp rate and total heat input. The solution macro increments through each of the 1,216 weld nuggets, saving each of the solved time step results. These thermal time step results are fed into the mechanical analysis as loading inputs much the same way that the thermal analysis uses the heat arrays as loading.

### Results of the Three-Dimensional Thermo Mechanical Analysis

The initial 2D analysis revealed maximum equivalent stresses of 45.8ksi. As can be seen in Figure 9, the 3D analysis also produced comparable results of approximately 43.6ksi.

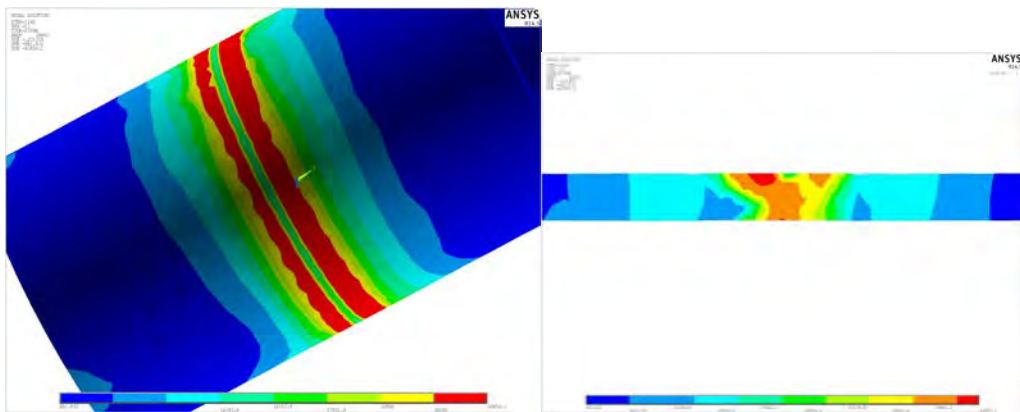


*Figure 9: Von Mises Stress and Cross-section Von Mises Stress.*

The axial and hoop stresses shown in Figure 10 did not produce smooth patterns or believable results. This is believed due to the coarseness of the mesh in the HAZ as well as the stiffness of the tetrahedral elements.



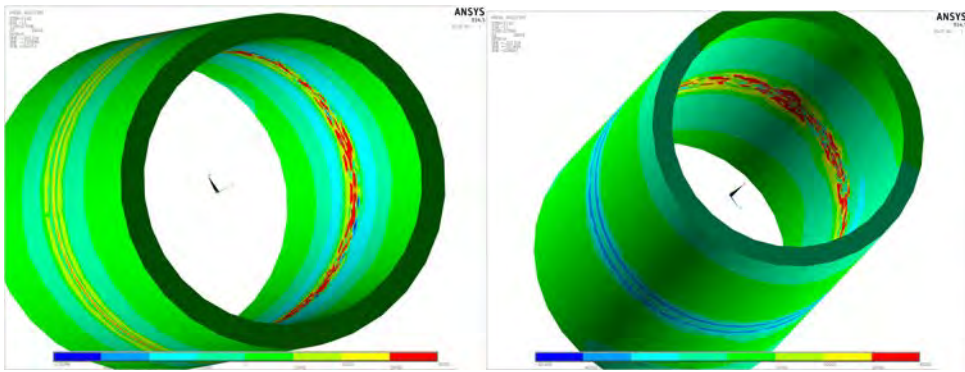


Figure 10: Axial Stress and Hoop Stress.

With the initial 3D analysis complete, a sensitivity study needs to be done to discover how much detail can be removed or needs to be added to retain sufficient accuracy to be used to analyze the effects of SCC. These initial results show that more fidelity is needed in the HAZ. This will be accomplished by extending the fine detailed mesh in the weld zone out further through the HAZ. Tetrahedral elements will be kept away from the areas of interest. The model will be further reduced by taking advantage of the axial symmetry and processed as a half model. Stress distribution changes due to cracking can then be introduced by freeing boundary constraints along the symmetry line thus simulating crack propagation.

Other possible areas to explore to reduce computing time would include combining multiple passes into a single lumped pass, taking advantage of lateral symmetry, or applying single weld passes at once instead of simulating a moving welding arc.

## CONCLUSIONS AND FURTHER WORK

In summary there are three distinct types of strain/cracking event that have been detected in this experiment:

- Initiation of SCC cracking in the form of an approximately  $60\text{-}\mu\epsilon$  spike in strain in all gages, similar to that observed in previous EDM experiments.
- Steady state crack growth indicated by a gradual and sustained divergence from the baseline strain.
- Start/stop or “pop” crack growth characterized by “hat shaped” strain profiles as a crack progresses through a localized region of lower toughness, and then arrested once it progressed through this region.

It is also evident from the complexities of crack interaction observed in this more realistic simulation of SCC that it would be highly challenging to correlate crack depth and location around the circumference with strain response. However, sharp changes in slope in the strain response may still be distinguished and flagged as a crack initiation/growth event for further inspection.

The main conclusions from the initial results of the weld simulation model were:

- We have successfully developed and documented a procedure for analyzing weld residual stresses using the ANSYS finite element software package. A complete set of input macros have been written to allow for easily changing the parameters such as weld and piping dimensions, number of weld beads, heat input, meshing of the model, and solving. Comparative studies can now be efficiently solved and analyzed.
- The axial and hoop stresses did not produce smooth patterns or believable results due to mesh coarseness in the HAZ and the stiffness of the tetrahedral elements.
- A sensitivity study should be performed to ascertain the level of detail that can be removed or needs to be added to retain sufficient accuracy to be used to analyze the effects of SCC.
- A greater degree of fidelity is required in the HAZ. This will be accomplished by extending the fine detailed mesh in the weld zone out further through the HAZ. Tetrahedral elements will be kept away from the areas of interest.
- The model will be further reduced by taking advantage of the axial symmetry and processed as a half model.
- Once fidelity has been improved, stress distribution changes due to cracking may then be introduced by freeing boundary constraints along the symmetry line thus simulating crack propagation.

This experiment has confirmed that it is possible to generate real SCC cracks on a large scale. They can be detected using fiber optic strain gages monitoring the change in residual stress on the OD of a pipe section as a result of ID initiated SCC cracks. The strain events are all characterized by an abrupt change in strain with respect to time. Such an abrupt change is unlikely to be due to external events in a plant. In order to automate cracking event detection, data could be analyzed by taking a running average of the data to reduce noise, then taking its first derivative. The sharp changes of slope associated with strain events will then be flagged in a first derivative of strain response vs. time plot. The results of this and future large scale SCC experiments will then be used to calibrate the weld simulation model. This model may then be used and adapted to simulate a variety of damage mechanisms and geometries.

## REFERENCES

- [1] Jackson, B., "Interim Status Update: EDM Crack Simulations," (2010) *EPRI Project Status Report AES 10067465-2-1*.
- [2] Jackson, B. *et al*, "Detection of Incipient SCC Damage in Primary Loop Piping using Fiber Optic Strain Gages," (Orlando, FL, 2011) *EPRI Conference: Welding and Fabrication Technology for New Power Plants and Components*.
- [3] Jackson, B. *et al*, "Detection of Incipient SCC Damage in Primary Loop Piping using Fiber Optic Strain Gages," (Columbus, OH, 2011) *MS&T2011*.
- [4] Hickling, J. *et al*, "Status Review of Initiation on Environmentally Assisted Cracking and Short Crack Growth," (2005) *EPRI Report 10117888*.
- [5] "Standard Practice for Evaluating Stress-Corrosion-Cracking Resistance of Metals and Alloys in Boiling Magnesium Chloride Solution," (2013) ASTM G36-94.
- [6] "Materials Safety Data Sheet (MSDS) for Magnesium Chloride Hexahydrate (MgCl<sub>2</sub>·6H<sub>2</sub>O)," CAS# 7791-18-6, ACC# 13365, Revised 8/20/2000.